Modeling and control of ship propulsion with shaft generator and battery storage system

Fan Gao, Astrid H. Brodtkorb, Mehdi Zadeh
Department of Marine Technology, Norwegian University of Science and Technology (NTNU).
Trondheim, Trøndelag, Norway

ABSTRACT

The use of shaft generators in marine applications makes it possible to operate the main engine more efficiently and to provide additional power to the electrical system. This paper develops a dynamic model and controller for a hybrid marine propulsion system that operates efficiently in both mechanical and hybrid modes such as power take-off (PTO). A simplified electric power system model with a shaft generator and a battery set is introduced into the ship propulsion system. The corresponding control and switching logics are also described and are proved with simulations.

KEY WORDS: Ship propulsion; shaft generator; controllable -pitch propeller; mode switching; marine batteries.

INTRODUCTION

Nowadays, hybrid ship propulsion systems are of great interest and the application of shaft generators (SGs) has developed rapidly. The operation mode of a hybrid ship propulsion system can include power take-in (PTI), power take-off (PTO), and boost mode (Sui, de Vos, Stapersma, Visser, and Ding, 2020). In this paper, we investigate the use of optimal combinator curves for the control of a hybrid ship propulsion system driven by an engine with and without a shaft generator.

For marine applications, the main propeller can be driven by the engine, and the shaft generator can be engaged to charge the battery set and/or power the electric bus (PTO mode). Using the shaft generator system to charge the battery is more efficient than starting auxiliary engines (Liu, Xue, and Ye, 2007; Prousalidis, et al., 2012; Sarigiannidis, Kladas, Chatzinikolaou, and Patsios, 2015). Fig. 1 shows an overview of the proposed propulsion system, which consists of a main diesel engine (DE), a controllable pitch propeller, and a shaft generator (SG) connected to the electric system (EL).

Since many combinations of shaft speed and propeller pitch can produce the same thrust, the propulsion control problem with controllable pitch propeller (CPP) (Carlton, 2018) can be formulated as the optimization of a cost function. For example, many marine propulsion control systems focus on reducing fuel consumption and avoiding cavitation at the propellers. The combinator curve set used in this report is optimized for maximizing efficiency. The optimal setpoints of propeller pitch and shaft speed are chosen from the optimal combinator curve and are controlled independently.

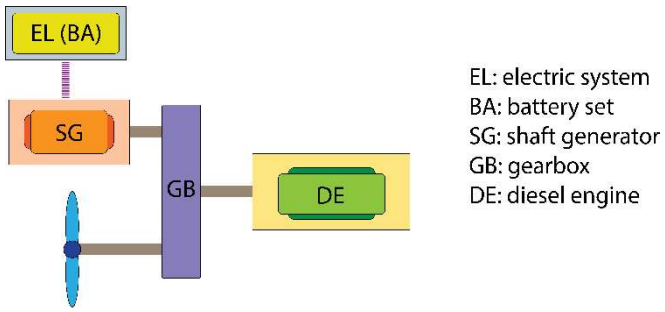

Figure 1. Simplified diagram of the ship hybrid powertrain.

Mathematical modeling of marine diesel engines is performed with varying fidelity for different purposes. For the purpose of higher level controller simulation and testing, Fossen (2011) models the prime mover system as a first-order transfer function with a time delay. The control input to the engine system can be the fuel injection for the diesel engine or the power required for the electric propulsion system to produce the desired torque. These models do not account for the dynamics of marine power systems. For diesel engines, load control is achieved by changing the fuel injection in each cycle. Vrijdag and Stapersma (2017) explain the reason for the time delay in engine modeling, claiming that the conversion from fuel injection command to actual fuel injection takes a maximum of two revolutions for a four-stroke diesel engine. Altosole and Figari (2011) present three options for numerical modeling of marine engines: Modeling using mathematical equations, numerical surfaces, and PI action. Altosole, Campora, Figari, Laviola, and Martelli (2019) present a high-fidelity model of the thermodynamic behavior of diesel

engines. In this work, the diesel engine model proposed by Fossen (2011) is used for the mechanical system, since the time constant of the mechanical system is much larger than that of the electrical system.

Shaft generators are typically used to generate electrical power for ships with a propulsion system in which the shaft system is driven by the main engine. Some advantages of using shaft generators are: High reliability, low installation and spare part costs, and they enable high efficiency of the diesel engine under part-load conditions (Sarigiannidis, Patsios, Kakosimos, and Kladas, 2012). For ships equipped with a controllable pitch propeller, an efficient combinator control system can be used with the implementation of a shaft generator.

A synchronous machine is often used as the shaft generator, which can run at a fixed speed regardless of its load. The induced voltage of the shaft-driven generator can be regulated by changing the excitation current. On the one hand, the shaft generator can be connected to the bus directly, and the generated voltage and frequency must match the required bus voltage and frequency. On the other hand, if the shaft system rotates at different speeds, a chain of rectifier and DC /DC converter needs to be implemented. In this paper, the power output from the shaft generator is sent directly to bus. Under PTO mode, the induced voltage of the shaft generator is controlled to maintain the bus voltage/terminal voltage, while a battery is used to absorb the energy generated by the shaft generator and maintain the system frequency. Bø, et al. (2015) proposed a power-based electric bus model for ship power and propulsion. Synchronous generators are used for power generation and modeled at steady state.

The torque angle, defined by the phase difference between the terminal voltage and the induced voltage, increases with the applied load. When the torque angle increases to 90 degrees, the synchronous machine delivers the maximum torque (Veltman, Pulle, and De Doncker, 2007). In AC systems, the power factor is used to represent the relationship between the power absorbed by the loads and the apparent power flowing in the circuit. The sign of the power factor is determined by the direction of the active power. The power factor is negative when the machine under consideration is generating current. If, on the other hand, the machine draws current, the power factor is positive.

However, the use of a shaft generator poses a challenge to electrical stability. Changes in power demand and its rate of change can be large for the electrical system onboard (Skjong, Taskar, Pedersen, and Steen, 2016). The energy storage device (e.g., a battery set) can compensate for the fluctuating electricity demand. The concept of using battery storage for propulsion was first introduced to use batteries to store braking energy, run the engine efficiently, and to enable switching off the engine. It has been shown that optimizing battery use with smart control strategies can lead to a 10-35% reduction in fuel consumption and emissions (Geertsma, Negenborn, Visser, and Hopman, 2017). Hansen and Wendt (2015) note that the energy storage system can perform a wide range of functions, including spinning reserve, peak shaving, improved dynamic performance, and strategic loading. To safely deploy the battery in a marine propulsion system, Bø and Johansen (2016) use battery temperature and state of charge (SoC) to limit the rate of charging and discharging rate, and mode switching.

In low to mild sea states with limited wave heights, the encounter frequency of waves is high for short head waves, so the wave-induced surge motions can be neglected and the additional resistance of the ship due to waves is dominated by the wave reflection of the hull at the waterline. Taskar, Yum, Steen, and Pedersen (2016) study the effects of waves on the propulsive performance of ships and claim that accurate estimation of wake fluctuations is essential for estimating ship performance. Nakamura and Naito (1977) conclude that the fluctuations of propeller thrust, and torque are mainly caused by the fluctuation of axial inflow velocity in the propeller disk. Changes in the wake component in heading waves and ship pitch motions are estimated using the formulas in Ueno, Tsukada, and Tanizawa (2013) and Faltinsen (1980). Ueno, Tsukada, and Tanizawa (2013) also state that the effects of oscillation of the propeller position or pitch and heave motion are found to be negligible by experimental calculations. The wake changes were considered in the quasi-steady sense since the propeller depth varies much more slowly than the rotational speed.

In this paper, a switching strategy between mechanical and PTO operation is proposed for a hybrid ship propulsion system. The performance is discussed using time-domain simulations. The paper is organized as follows. Section 2 contains the problem formulation and modeling method for the entire propulsion system. Section 3 presents the controller design and switching logic of the target system. Section 4 contains the simulation and discussion of the proposed hybrid ship propulsion system, and in Section 5 we conclude the paper.

SYSTEM MODELING

The dynamics of the ship propulsion system contain the propeller shaft dynamics (Eq. 1), including loads from the diesel engine, shaft generator, wherein the electric system enters, the propeller and frictional losses.

$$J_s\dot{\omega} = M_E + M_{SG} + M_P + M_F \tag{1}$$

where J_s is the moment of inertia sum of the shaft system. ω is the shaft rotating speed. M_E, M_{SG}, M_P and M_F are diesel engine (DE) provided torque (Eq. 4), shaft generator (SG) torque (Eq. 9), propeller torque (Eq. 11), and frictional torque (Eq. 15) of the shaft system. Due to gear implementation, the output torque from the diesel engine is different from the shaft torque delivered by the diesel engine, and the same is true for SG. The gear ratio between engine shaft and propeller shaft, and between SG shaft and propeller shaft are 4.121 and 6.593, respectively.

The advance speed of the ship must be estimated for proper propulsion modeling, and therefore a simplified ship model (Eq. 2) is also included.

$$M\dot{V} = F_P - F_R - F_E \tag{2}$$

where F_P is the thrust provided by the propeller (Eq. 12), F_R is the resistance of the ship in the calm water, and F_E is the added resistance due to waves. The ship resistance F_R is mainly determined by the ship speed, and the underwater hull profile. The ship resistance is modeled using a polynomial function of ship speed V (Eq. 3) (Zhao, Yang, Zhou, Li, and Yang, 2018; Figari and Altosole, 2007). Coefficients A_i can be estimated using model test or sea trial data of the targeting ship if available.

$$F_R = A_1V + A_2V^2 + A_3V^3 + A_4V^4 + A_5V^5 + A_6V^6 \tag{3}$$

Diesel Engine

The torque produced by the ship engine can be approximated by a first-order system $H(s)$ with time delay (Fossen, 2011).

$$H(s) = \frac{M_E(s)}{X(s)} = \frac{K}{Ts+1}e^{-\tau s} \tag{4}$$

where τ represents the time delay, K is the gain constant, and T is the

time constant. This model is used to describe the diesel engine dynamics since the time constant of the mechanical system is much larger than that of the electric system. The control input $X(s)$ is the fuel injection command, see (Eq. 16). In a real implementation, the controller should limit the rate of change of the generated torque to prevent damages to the engine.

Electrical System

In this paper, it is assumed that power generated from the shaft generator is sent to the bus directly and is used to charge the battery. We use a synchronous machine as shaft generator. Physically, to charge the battery, rectifier and DC/DC converter are needed to transfer AC power to desired DC power. In this paper, we model the battery as a power storage unit (for PTO mode). The conversion between DC and AC, and the DC/DC conversion are neglected.

The synchronous machine is featured by consistent frequency of AC supply and the rotor rotating speed, and the relationship is formulated as

$$n = \frac{2 \cdot 60 f}{p} \tag{5}$$

where n is the SG rotating speed in rpm, f is the frequency in Hz, and p is the number of poles. For accurate modeling of a generator, seven degrees of freedom model must be applied, but for control purpose analysis, the generator is represented as a voltage source (E) with an inductor and a resistor (Z). Fig. 2 shows the per phase diagram of the shaft generator connected with varying loads.

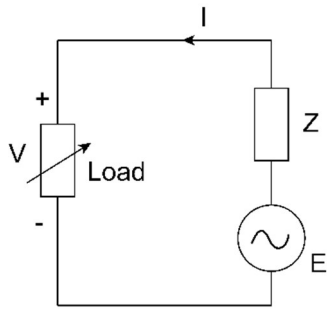

Figure 2. Circuit diagram of the bus with electric load and shaft generator.

The resulting power balance in the diagram can be formulated as

$$P + jQ = 3VI^* \tag{6}$$

where P and Q are total active and reactive power of bus, and j is the imaginary number $\sqrt{-1}$. V is the bus voltage per phase, and I is the phase current. The stator voltage equals to the induced voltage minus voltage drop over stator impedance Z. E is the generator-induced voltage per phase.

$$E = V + ZI \tag{7}$$

The induced voltage in the shaft generator is proportional to the SG rotating speed (ω_{SG}) and the field voltage. The average voltage regulator (AVR) regulates the terminal voltage of the shaft generator by controlling the field voltage (Bø, et al., 2015). The phase of SG comes from the integration of the difference between the SG frequency and bus frequency (Krause, Wasynczuk, Sudhoff, and Pekarek, 2013). In this paper, we only take the shaft generator as the power source to the bus, and thus the SG frequency is equivalent to the bus frequency. The impendence of shaft generator is

$$Z = R + j2\pi f L \tag{8}$$

where R, L, and f are the stator resistance, the synchronous reactance, and the shaft generator frequency respectively.

The battery is modeled as a power absorber under PTO mode, which should follow the guideline of the optimal combinator curve. The efficiency of the battery charging and discharging is not considered in this paper. We simplify the changes of desired power absorption by setting it as a constant. The power generated by the shaft generator is dependent on the charging rate of the battery set. The shaft generator torque is calculated as

$$M_{SG} = \frac{P + P_{loss}}{\omega} = \frac{P + RI^2}{\omega} \tag{9}$$

In the electric modeling, a per unit system is used, where system variables are expressed as fractions of defined base unit quantities. Base power and base voltage are firstly selected, and all parameters and variables are normalized using these base quantities (Krause, Wasynczuk, Sudhoff, and Pekarek, 2013). The SG rotating speed is converted to per unit by defining

$$\omega = \frac{\omega_{SG}}{\omega_{SG,b}} \tag{10}$$

where $\omega_{SG,b}$ is the base angular velocity of SG and ω_{SG} is the actual angular velocity of SG.

Propeller

This paper considers the ship propulsion system equipped with one main controllable-pitch propeller. The propeller thrust F_P and torque M_P are nonlinearly dependent on blade number (z), advance number (J), pitch angle (P_p), propeller diameter (D), propeller expanded blade area ratio (A_E/A_O), and Reynolds number (R_n).

$$M_P = K_Q \rho n^2 D^5, \quad K_Q = f_Q\left(z, \frac{P_P}{D}, J, \frac{A_E}{A_O}, R_n\right) \tag{11}$$

$$F_P = K_T \rho n^2 D^4, \quad K_T = f_T\left(z, \frac{P_P}{D}, J, \frac{A_E}{A_O}, R_n\right) \tag{12}$$

where K_T and K_Q are propulsion coefficients. The advance number $J = V_a/nD$, where V_a is the inflow velocity and n is the propeller rotating speed in rps. To demonstrate the propeller inflow disturbances due to waves, Taskar, Yum, Steen, and Pedersen (2016) and Ueno, Tsukada, and Tanizawa (2013) formulate the wake velocity (inflow velocity V_a) as

$$V_a = (1 - w_p)\left[V - \omega_e \zeta_a \sin(\omega_e t - \varepsilon_\zeta)\right] + \alpha \omega h_a e^{-kz_p} \cos\chi \cdot \cos(\omega_e t - k x_p \cos\chi) \tag{13}$$

where w_p is the wake fraction in calm water, ω_e is the wave encounter frequency, ζ_a is the surge motion of the ship, ε_ζ is the phase delay, χ is the wave encounter angle, and k is the wave number. x_p and z_p demonstrate the propeller position in longitudinal and horizontal directions. ITTC (2017) claims that in low to mild sea states with restricted wave heights, the wave induced motions can be neglected in short head waves since the encounter frequency of waves is high. Thus, the wave-induced surge motion ζ_a is neglected.

For controllable pitch propeller, Geertsma, Negenborn, Visser, Loonstijn,

and Hopman (2017) states that a first order linear system can demonstrate the overall pitch behavior including friction, oil leakage, pressurizing and inertia in the pitch actuation system. In this paper, the propeller pitch is modeled using the following equation:

$$\frac{dP_P}{dt} = \frac{P_{P-d} \quad -P_P}{\tau_P} \tag{14}$$

where P_P is the actual propeller pitch, P_{P-des} is the desired pitch setpoint from the controller, and τ_P is the time constant of the pitch model.

Shaft Friction

The frictional torque tends to be proportional to the engine rotating speed with static friction, that is

$$M_F = sign(\omega)M_{F0} + K_F\omega \tag{15}$$

where $sign()$ is the sign function. The friction term is less significant on large thrusters used on surface vessels than on small thrusters typically used on underwater vehicles. In this paper, static friction M_{F0} is neglected.

SWITCHING LOGICS AND CONTROLLER DESIGN

Switches are assumed to be done manually between mechanical propulsion and PTO modes. Fig. 3 shows the electrical system with connection to the shaft system via shaft generator under PTO mode. The shaft generator is connected to the bus directly and operates at constant speed. Other loads could be added to the bus as power absorbers as well.

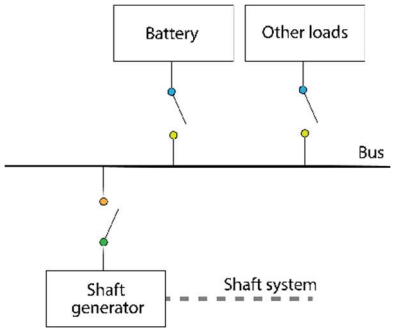

Figure 3. Representation of the electric power system.

Diesel Engine Control

The trade-off between avoiding engine overloading and increasing maneuverability is intuitive. Too fast dynamics in engine speed may induce overloading of shaft torque. In the engine speed dynamics design, the control objective is to minimize the error between the actual engine speed and the desired engine speed as soon as possible while keeping each system variable in a safe region and limiting oscillations. The control output X is the engine fuel injection per cycle. The PI controller is widely adopted in the control design. To restrict the maximal and minimal fuel injection and its rate, a limitation is added on the fuel injection. Correspondingly, an anti-windup design is proposed to avoid integral windup. Anti-windup is previously applied in the integrating action of shaft speed control (Izadi-Zamanabadi and Blanke, 1999). The fuel injection output X from the engine controller can be expressed as

$$\begin{aligned} X &= sat(X_b) \\ X_b &= K_p(\omega_{des} - \omega) + \zeta_\omega \\ \dot{\zeta}_\omega &= K_i(\omega_{des} - \omega) - K_a(X_b - X) \end{aligned} \tag{16}$$

where ω_{des} and ω are the desired and actual shaft speeds. X_b is the PI-controlled fuel injection before the anti-windup operation. The anti-windup operation regulates the lower- and upper- limit of the PI fuel injection via changing the integral control ζ_ω. K_p, K_i, and K_a are proportional, integral, and anti-windup control coefficients. Fig. 4 shows the fuzzy logic-based PI controller design with anti-windup. The PI control gains are adjusted by the fuzzy logic. If the shaft speed difference is large, high PI control gains are used, and vice versa. The application of fuzzy logic (Sivanandam, Sumathi, and Deepa, 2007) enables smooth transitions between high and low gains.

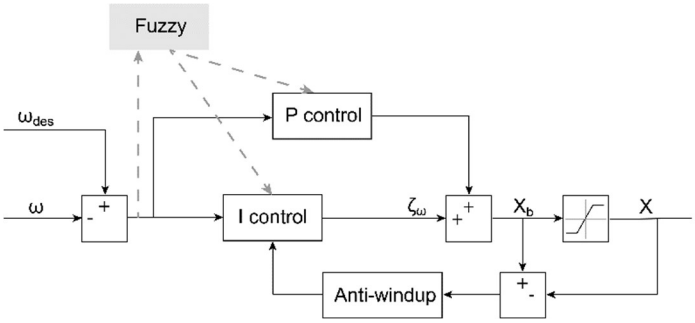

Figure 4. Representation of diesel engine controller.

Electric System

For PTO mode, the shaft generator rotating speed should be controlled to maintain around the '60Hz' frequency for the bus. It is assumed that the necessary power of the bus from other loads and battery set is constant, and the battery will regulate its charging rate if the bus frequency exceeds the margin. A dead zone block is implemented in the controller. The controller uses P control to help maintain the bus frequency deviation within the tolerable margin.

$$P = \begin{cases} P_{set} & |f - f_0| \le c \\ P_{set} + k(f - f_0) & |f - f_0| > c \end{cases} \tag{17}$$

where P_{set} is the predefined power absorbing of the battery set. f and f_0 are the actual and desired electrical frequency. The actual electrical frequency is proportional to the shaft generator rotating speed. If the frequency deviation exceeds a constant c, the charging rate will be modified to reduce this deviation. Besides, providing that the power consumption of the bus is only supplied by the shaft generator, the bus frequency is consistent with the synchronous shaft generator frequency. The induced voltage in the windings of the shaft generator is proportional to the rotating speed of the magnetic flux and the magnitude of the magnetic flux. In steady state, the rotating speed of the magnetic flux equals the rotating speed of the rotor. The induced voltage is controlled to maintain the bus voltage level using a P control. Due to the simplification of AC-DC conversion as proposed before, the battery set is regarded as a power absorb device and energy loss is not considered.

To sum up, an anti-windup PI controller is applied to the diesel engine to control the shaft rotating speed. Propeller pitch is controlled using P control strategy. The combination of desired shaft speed and propeller pitch is assumed known from optimal combinator curves. The electric system absorbs power for battery charging and other loads. This paper

does not focus on how efficient the power conversion is or how much power is needed instantaneously by the ship electric system. We concentrate rather on the hybrid modeling and control of the propulsive shaft system and simplify the electric system to be one input to the shaft system. For further work, the electric part can be extended to a complete electric system taking load-sharing amongst gensets, efficiency of power conversion, and power management system into consideration.

SIMULATION AND ANALYSIS

Simulation setup

The simulation is performed with switching between mechanical propulsion and PTO modes. Table 1 shows the available switching modes. An additional switching mode (SC) is implemented to control the switches. Even though the mode command is updated, the actual mode does not change until the operating conditions meet the requirements for mode switching. The SC mode takes control of the main propeller pitch position and shaft speed during the switch. The desired pitch position is zero and the desired generator speed is 1200 rpm. The controller allows a small margin for the changeover, usually 10% offset.

Under mechanical propulsion (Mode 0), the setpoints of shaft speed and pitch position are derived from the combinator curve with desired thrust force from higher-level ship speed control. The shaft rotating speed is controlled by varying the fuel injection to the diesel engine. The shaft generator is not engaged to the shaft system. For PTO mode, the shaft generator is connected to the bus directly. To avoid damaging the shaft generator and the whole electric system, the engine is set to a pre-set RPM under PTO mode. The combinator lever controls only the propeller pitch.

Table 1. Modes definition for controller

Mode 0	Mechanical propulsion using DE
Mode 2	PTO using DE as the power source for both propulsion and SG
Mode 10 Switch control (SC)	Switching mode: After changes on the commanded switch, this mode executes constant shaft speed and zero propeller pitch commands until the system fulfills all switching requirements.

Hybrid ship propulsion simulation

The simulation was done with switches between Mode 0 (Mechanical propulsion) and Mode 2 (PTO). The desired setpoints of shaft speed and pitch angle are listed in Table 2. We assume long-crested head sea waves with wave height 1m and wavelength 15m during simulation. The wave-induced added resistance is also introduced into the plant model using ITTC (2017).

Fig. 4 shows the commanded, controlled, and actual mode changes during the simulation. The commanded one is derived directly from the mode selection, and the controlled one is used in the controller for setting up desired setpoints of shaft speed and propeller pitch. The desired shaft speed and propeller pitch angle in the controller are defined by switching criteria and not by the optimal combinator curve during the switching control mode. The 'Actual' mode indicates which mode is currently being executed by the propulsion system. The shaft speed and propeller pitch angle must meet the switching criteria before switches occur. It can be observed that the SC mode takes around 50 seconds between mode changes. The length of the SC period depends not only on the control parameter settings but also on the previous operating conditions of the shaft system.

Table 2. Mode switches during simulation

Time [s]	Mode	Shaft speed	Pitch
0-400	0	133 RPM	3m
400-800	2	182 RPM	2.2m
800-1200		182 RPM	2.6m
1200-1600	0	158 RPM	2.5m

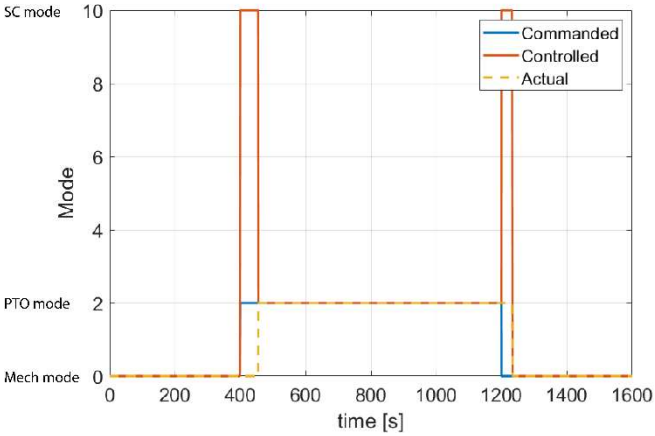

Figure 4. Plot of the commanded, controlled, and actual modes in simulation. Commanded: Set as described in Table 2; Controlled: modes used in the controller as described in Table 1; Actual: modes that are used in the ship propulsion system.

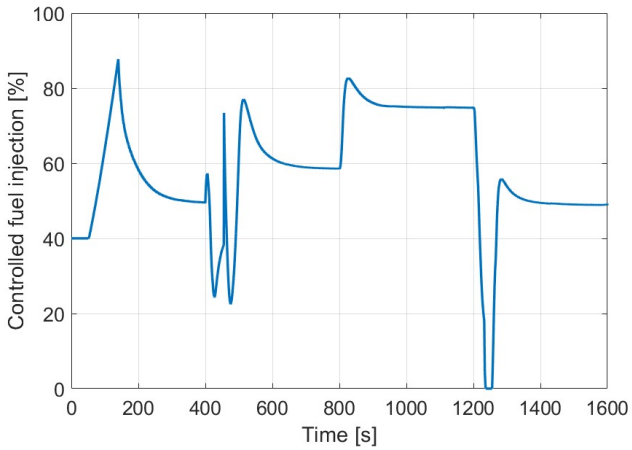

Figure 5. Plot of the fuel injection from engine controller.

Fig. 5 shows the fuel injection value calculated by the diesel engine controller. The desired shaft speed is set by a rate limiter before it is sent to the controller. The maximum fuel injection is used for acceleration during startup and when switching to another mode that requires high propulsion power. If the gain of the PI controller is increased, the diesel engine can accelerate or deaccelerate the shaft system quickly, but the resulting fuel injection can be unnecessarily high for a short period of time, causing the system to overload.

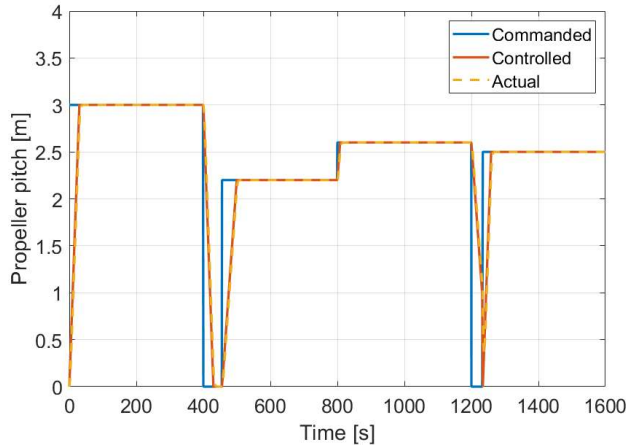

Figure 6. Plot of the commanded, controlled, and actual propeller pitch angle.

Fig. 6 shows the commanded, controlled, and actual propeller pitch. The control of the propeller pitch is much faster than that of the shaft system and is independent of the shaft system. We included a rate limiter in the pitch controller to avoid abrupt changes in propeller load. Fig. 7 shows the commanded and actual shaft rotating speed in different propulsion modes. In PTO (Mode 2), the shaft generator transfers mechanical power into electrical power. Physically, one can regulate the torque of the shaft generator by controlling the charging rate of the battery. The control uses the concept of dead zone, which is defined by the deviation between the desired and the actual SG speed, and the battery charging rate is adjusted outside the predefined dead zone. The battery charging is controlled to balance the electrical frequency as shown in Fig. 8. When the SG speed deviation is within the dead zone, the charging rate remains constant at about 90 kW. The wake-induced oscillations of the shaft speed are not introduced into the electrical system by using the dead zone block in the simulation.

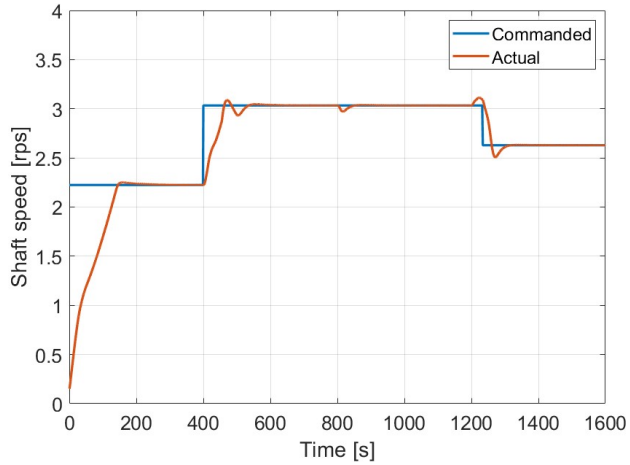

Figure 7. Plot of the commanded and actual shaft rotating speed.

Reference tracking of shaft speed and propeller pitch is shown in Fig. 6 and Fig. 7. The performance of the tracking is satisfactory. As mentioned for diesel engine control in Section 3, the shaft system is large and the tradeoff between fast maneuverability and avoiding overload, limits the rate of change of shaft speed. It is assumed that the setpoints of shaft speed and propeller pitch angle are known, but for further work, the setpoint selection design could be developed based on higher-level controllers (such as the ship speed controller) and the optimal combinator curve sets.

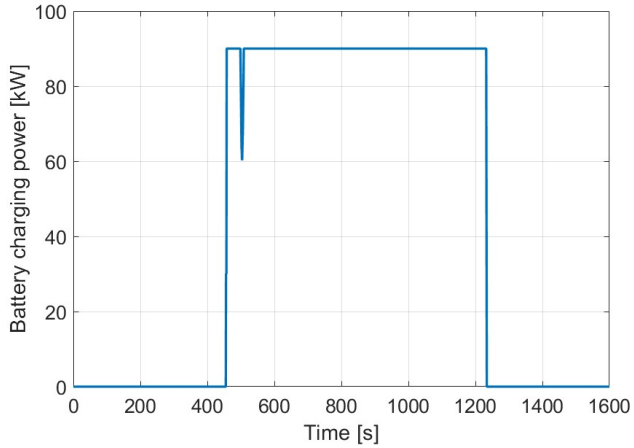

Figure 8. Plot of battery charging power in simulation.

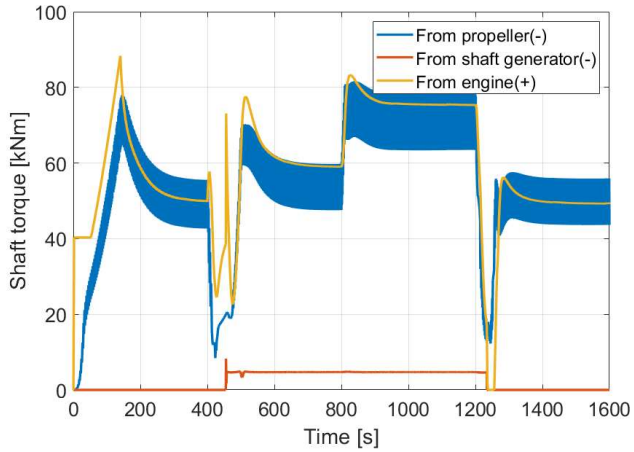

Figure 9. Plot of shaft torques from the diesel engine, the shaft generator, and the propeller.

Fig. 9 presents the shaft torques from the diesel engine, the shaft generator, and the propeller. The diesel engine provides the torque for the shaft system, while the shaft generator and propeller consume torques. Due to the gear ratio, the first two torques do not correspond to the actual torque generated by the engine and the torque from SG. From Fig. 9, the engine torque changes abruptly during the mode change and setpoint changes because the propeller torque changes suddenly due to a large change in pitch angle, and the shaft speed increases before the PI engine injection control responds. The overshoot of the PI controller could be reduced by introducing derivative control. However, the fact is that wake-induced disturbances are introduced into the system. In addition, high-frequency oscillations of the shaft system may injure the engine if D control is introduced. Increasing the derivative gain increases unnecessary fuel consumption to compensate for oscillations and shaft disturbances, which is not desirable. Another way to reduce the severe oscillations of the engine torque is to limit the pitch change rate so that the entire system can respond smoothly during mode changes.

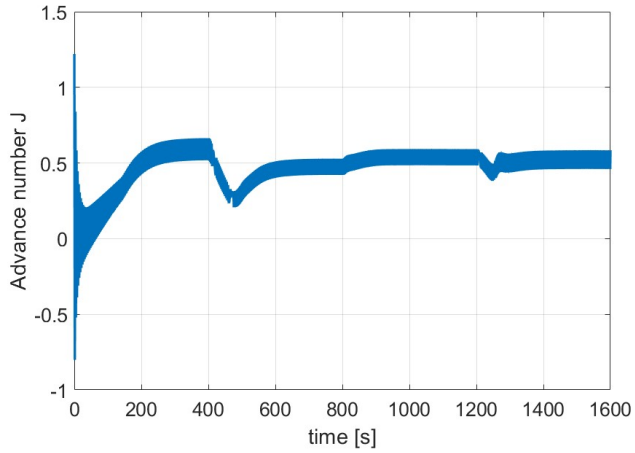

Figure 10. Plot of the advance number.

Fig. 10 shows how the advance number oscillated with the encounter frequency of the waves, introducing vibrations into the shaft system. The wave encounter frequency depends on the wave frequency, ship speed, and the relative direction of the ship's course compared to the wave direction. For head sea waves, the vibration frequency increases with ship speed and wave frequency. In this work, the wave-induced surge motion of the ship is not included in simulations.

Fig. 11 shows the resulting ship speed during operation time. It is varying by the variations in the shaft rotating speed and propeller pitch position. This paper focuses on the control of ship power and propulsion system, and whether the ship achieves its 'expected speed' from combinator curve is out of the research scope.

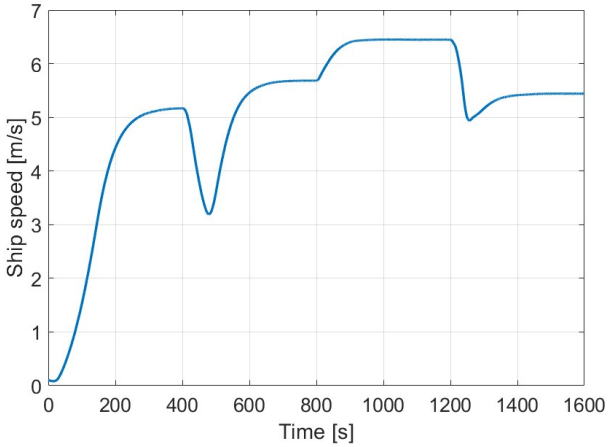

Figure 11. Plot of the ship velocity during the operation time.

In summary, the performance of the proposed control strategy was tested with the hybrid ship propulsion system and mode switching was performed during the simulations. The PI controller with anti-windup shows good performance in controlling the fuel injection of the engine. The battery controller used in this work maintains the charge rate during ship navigation and supports faster mode switching, acceleration and deceleration by controlling the charge rate.

CONCLUSION

This paper presents the modeling and controller design of a hybrid marine propulsion system with mode switching between mechanical propulsion and PTO. The main contribution is the system modeling and fuzzy controller design of the ship propulsion system and the simplification of the electrical system together with its integration with the mechanical part via the shaft generator. The ship thrust and resistance, and balance of the shaft system are formulated with detailed models of the diesel engines, the electrical system with battery set and shaft generator, and the controllable pitch propeller. The simulation was performed in Simulink and the case study shows balanced shaft dynamics between the diesel engine, shaft generator, and propeller. Further work will focus on the optimization of the combinator curve and its implementation in the proposed propulsion system.

ACKNOWLEDGEMENTS

This work was supported by the Research Council of Norway through the IPN-SEAOPS project of Brunvoll AS, project number 309660, and by the Centre of Excellence funding scheme, project number 223254, AMOS. We thank the SEAOPS project partners and Dr. Torstein I. Bø from SINTEF Ocean AS for valuable discussions.

REFERENCES

Altosole, M., and Figari, M. (2011). Effective simple methods for numerical modelling of marine engines in ship propulsion control systems design. *Journal of Naval Architecture and Marine Engineering*, 129-147.

Altosole, M., Campora, U., Figari, M., Laviola, M., and Martelli, M. (2019). A diesel engine modelling approach for ship propulsion real-time simulators. *Journal of Marine Science and Engineering*, 138.

Bø, T. I., and Johansen, T. A. (2016). Battery power smoothing control in a marine electric power plant using nonlinear model predictive control. *IEEE Transactions on Control Systems Technology*, 25(4), 1449-1456.

Bø, T. I., Dahl, A. R., Johansen, T. A., Mathiesen, E., Miyazaki, M. R., Pedersen, E., . . . Yum, K. K. (2015). Marine vessel and power plant system simulator. *IEEE Access*, 2065-2079.

Carlton, J. (2018). *Marine propellers and propulsion.* Butterworth-Heinemann.

Faltinsen, O. M. (1980). Prediction of resistance and propulsion of a ship in a seaway. *In Proceedings of the 13th symposium on naval hydrodynamics.* Tokyo.

Figari, M., and Altosole, M. (2007). Dynamic behaviour and stability of marine propulsion systems. *Proceedings of the Institution of Mechanical Engineers, Part M: Journal of Engineering for the Maritime Environment*, 221(4), 187-205.

Fossen, T. I. (2011). *Handbook of marine craft hydrodynamics and motion control.* John Wiley & Sons.

Geertsma, R., Negenborn, R., Visser, K., and Hopman, J. (2017). Design and control of hybrid power and propulsion systems for smart ships: A review of developments. *Applied Energy*, 30-54.

Hansen, J. F., and Wendt, F. (2015). History and state of the art in commercial electric ship propulsion, integrated power systems, and future trends. *Proceedings of the IEEE*, 103(12), 2229-2242.

ITTC (2017). Recommended procedures and guidelines 7.5-04-01-01.1, preparation, conduct and analysis of speed/power

trials.
Izadi-Zamanabadi, R., and Blanke, M. (1999). A ship propulsion system as a benchmark for fault-tolerant control. *Control Engineering Practice*, 7(2), 227-239.
Krause, P. C., Wasynczuk, O., Sudhoff, S. D., and Pekarek, S. D. (2013). *Analysis of electric machinery and drive systems.* John Wiley & Sons.
Liu, Y., Xue, S., and Ye, Y. (2007). Development of a new-type shaft-driven generator. *International Conference on Electronic Measurement and Instruments* (pp. 1-422). IEEE.
Nakamura, S., and Naito, S. (1977). Propulsive performance of a container ship in waves. *Journal of the Society of Naval Architects of Japan*, 15.
Prousalidis, J., Patsios, C., Kanellos, F., Sarigiannidis, A., Tsekouras, N., and Antonopoulos, G. (2012). Exploiting shaft generators to improve ship efficiency. *Electrical Systems for Aircraft, Railway and Ship Propulsion*, 1-6.
Sarigiannidis, A., Kladas, A., Chatzinikolaou, E., and Patsios, C. (2015). High efficiency Shaft Generator drive system design for Ro-Ro trailer-passenger ship application. *International Conference on Electrical Systems for Aircraft, Railway, Ship Propulsion and Road Vehicles* (pp. 1-6). IEEE.
Sarigiannidis, A., Patsios, C., Kakosimos, P., and Kladas, A. (2012). Control design and performance analysis of shaft generators in ship power systems. *1st International MARINELIVE Conference on "All Electric Ship"*, (pp. 3-5).
Sivanandam, S. N., Sumathi, S., and Deepa, S. N. (2007). *Introduction to fuzzy logic using MATLAB.* Berlin: Springer.
Skjong, S., Taskar, B., Pedersen, E., and Steen, S. (2016). Simulation of a hybrid marine propulsion system in waves. *In Proc. 28th CIMAC World Congr*, (pp. 1-16).
Sui, C., de Vos, P., Stapersma, D., Visser, K., and Ding, Y. (2020). Fuel consumption and emissions of ocean-going cargo ship with hybrid propulsion and different fuels over voyage. *Journal of Marine Science and Engineering*, 8(8), 588.
Taskar, B., Yum, K. K., Steen, S., and Pedersen, E. (2016). The effect of waves on engine-propeller dynamics and propulsion performance of ships. *Ocean Engineering*, 122, 262-277.
Ueno, M., Tsukada, Y., and Tanizawa, K. (2013). Estimation and prediction of effective inflow velocity to propeller in waves. *Journal of Marine science and Technology*, 18(3), 339-348.
Veltman, A., Pulle, D. W., and De Doncker, R. W. (2007). *Fundamentals of electrical drives.* Power systems: Springer.
Vrijdag, A., & Stapersma, D. (2017). Extension and application of a linearised ship propulsion system model. *Ocean Engineering*, 50-65.
Zhao, Z., Yang, Y., Zhou, J., Li, L., and Yang, Q. (2018). Adaptive fault-tolerant PI tracking control for ship propulsion system. *ISA transactions*, 80, 279-285.